scientific reports

Check for updates

OPEN

Enhancing brain tumor classification through ensemble attention mechanism

Fatih CELIK[1]✉, Kemal CELIK[2] & Ayse CELIK[3]

Brain tumors pose a serious threat to public health, impacting thousands of individuals directly or indirectly worldwide. Timely and accurate detection of these tumors is crucial for effective treatment and enhancing the quality of patients' lives. The widely used brain imaging technique is magnetic resonance imaging, the precise identification of brain tumors in MRI images is challenging due to the diverse anatomical structures. This paper introduces an innovative approach known as the ensemble attention mechanism to address this challenge. Initially, the approach uses two networks to extract intermediate- and final-level feature maps from MobileNetV3 and EfficientNetB7. This assists in gathering the relevant feature maps from the different models at different levels. Then, the technique incorporates a co-attention mechanism into the intermediate and final feature map levels on both networks and ensembles them. This directs attention to certain regions to extract global-level features at different levels. Ensemble of attentive feature maps enabling the precise detection of various feature patterns within brain tumor images at both model, local, and global levels. This leads to an improvement in the classification process. The proposed system was evaluated on the Figshare dataset and achieved an accuracy of 98.94%, and 98.48% for the BraTS 2019 dataset which is superior to other methods. Thus, it is robust and suitable for brain tumor detection in healthcare systems.

Keywords Attention, Brain tumor, Classification, CNN, Deep learning

Abbreviations

Attn	Attention
AUC	Area under curve
lr	Learning Rate
ROC	Receiver operating characteristics
EA	Ensemble Attention
LGG	Low Grade Glioma
HGG	High grade Glioma

Abnormalities in the brain pose a significant threat to the human nervous system and overall health[1]. Brain tumors are particularly severe, stemming from the uncontrolled growth of destructive cells within the human brain. According to the cell structure and location, brain tumors are classified into different types by the World Health Organization and the American Brain Tumor Association. For example, glioma, meningioma, and pituitary tumors are all examples of this[2]. Approximately 150 different types of brain tumors have been identified in humans and can be further distinguished as benign or malignant[3]. Malignant tumors exhibit rapid growth and have the potential to metastasize to other organs, in contrast to the slower growth and localized nature of benign tumors[4]. Gliomas, meningiomas, and pituitary tumors are the most prominent cancerous tumors[5]. Gliomas originate from the brain's glial cells; meningiomas can develop on the membrane safeguarding the brain and spinal cord[1]; and pituitary tumors, characterized as benign, form in the glands responsible for producing essential hormones for the body.

In the clinical context, magnetic resonance imaging (MRI) is the most capable of noninvasive visualization of the functionality and anatomy of brain tumors[6]. These tumors may either originate inside the brain or stem from other parts of the body, subsequently metastasizing to the brain[7]. The development of benign or malignant tumors can arise from the dissemination of cells or tissues in neighboring areas, as well as from the brain cells themselves. Over 700,000 people are impacted by early-stage brain tumors, according to statistics from

[1]Department of Geomatic Engineering, Yıldız Technical University, Esenler, Istanbul, Turkey. [2]Department of Geomatics Engineering, Gumushane University, Gumushane, Turkey. [3]Gumushane University, Kelkit Aydın Dogan Meslek Yuksekokulu, Gumushane, Turkey. ✉email: F.alpcelik@gmail.com

the Central Brain Tumor Registry of the United States. Indicators of the symptoms of brain tumors include persistent headaches, changes in vision, seizures, problems with balance, changes in cognition and personality, and cognitive fluctuations. The manifestation of symptoms can differ depending on the type, location, and size of the tumor[8]. Meningiomas are non-cancerous brain tumors that arise from brain membrane tissues. Another distinctive type of tumor originates in the pituitary gland, a crucial brain organ. By recognizing these distinctive characteristics of brain tumors, medical professionals can accurately diagnose and address these conditions[9].

In the last few decades, in radiology, computed tomography, electroencephalography, ultrasonography, positron emission tomography, magnetic resonance imaging, and single-photon emission computed tomography are just a few of the recent imaging modalities that have emerged. These imaging modalities not only reveal intricate details of brain tumors but also assist doctors in accurately diagnosing tumors and determining appropriate treatment methods[10]. Among these imaging modalities, MRI is the most widely used for detecting brain tumors[11]. By offering excellent soft tissue contrast without subjecting patients to excessive ionizing radiation, MRI provides essential information regarding the size, shape, and location of brain tumors.

The diagnosis of brain tumors is a time-consuming process that relies heavily on the skills and knowledge of radiologists. With the increasing number of patients, the volume of data to be processed has surged, rendering traditional techniques costly and prone to errors[12]. Difficulties emerge because of shared symptoms across diseases and the fact that brain tumors can vary in size, shape, and intensity, even among types of brain tumors. Significant repercussions that affect patient survivability can result from the misclassification of brain tumors. The limitations of manual diagnosis have sparked increased interest in the development of automated image-processing technologies to address these challenges[10,13–16]. Consequently, various computer-aided diagnosis (CAD) systems have recently been developed to automate the detection of brain tumors. Identifying brain tumors poses a complex challenge because of their diverse shapes, intensities, sizes, and locations. Traditional methods involving visual inspection and manual marking are prone to errors attributed to blurred borders and subjective interpretation. Factors such as radiologist fatigue and noisy images further complicate accurate diagnosis. In response to these challenges, automated systems have been proposed to address issues such as determining the tumor depth and type, thereby reducing the need for invasive biopsies.

The two primary categories of computer-aided detection (CAD) methods are traditional machine-learning (ML) algorithms[17,18] and deep-learning-based methods. ML-based systems need to be segmented and features extracted manually like intensity, shape, and texture[57,59], but DL-based algorithms, particularly convolutional neural networks[19], can perform this automatically and perform well in medical image analysis. However, the current methods have limitations, including time-consuming and memory-intensive handcrafted features, complexities, fixed input image sizes, and high costs. It is still difficult to choose the best CNN model with the appropriate hyperparameters, and previous methods have failed because of numerous preprocessing steps.

The research is motivated by the desire to enhance the accuracy and effectiveness of brain tumor diagnosis using advanced deep-learning techniques. By surpassing the disadvantages of traditional methods in accuracy and reducing preprocessing steps, the study aims to enhance the classification process. This method not only aims for precise detection but also seeks to simplify medical decision-making and improve patient outcomes by providing more accurate diagnostic results.

The primary objective of this research is to solve these problems by reducing the number of pre-processing steps, choosing deep learning models with the correct hyperparameters, and using CNN-based classification as the main method.

To validate the effectiveness of the proposed method, we used quantitative measures to evaluate the model using a benchmark brain tumor dataset. The key contributions of this model are summarized as follows:

This study introduced novel approaches to enhance the accuracy of brain tumor classification. The approach involves an ensemble co-attention mechanism implemented in the MobileNetV3 and EfficientNetB7 networks at both the intermediate and final levels. These methods aim to extract local- and global-level features, thereby facilitating the precise identification of diverse patterns within brain tumor images. The attention mechanism plays a pivotal role by selectively emphasizing relevant features, leading to improved classification accuracy and reduced time consumption. The evaluation of the Fig share dataset demonstrated impressive accuracy. This method involves five main steps: normalizing the image intensity, augmenting the dataset, extracting features using MobileNetV3 and EfficientNetB7, and applying attention to these extracted features. The classification was performed using the SoftMax software. This approach achieves better performance in classifying brain tumors from MR images.

Compared with existing systems, the results demonstrate the adaptability of the proposed method. The remainder of this paper is organized as follows: The literature review, Sect. "Literature survey", the methodology is described in Sect. "Proposed system", and Sect. "Results and discussion" discusses the results and experiments. Finally, Sect. "Conclusions" presents the conclusions of this study.

Literature survey

Brain tumor classification relies predominantly on two main methodologies: machine learning and deep learning[20]. A wide variety of methods have been investigated in the field of machine learning, from decision trees and genetic algorithms to k-nearest neighbor (KNN) and support vector machines (SVM)[21–23]. Brain tumor classification was given a new twist by Cheng et al.[24], who focused on enhancing performance by augmenting the tumor region. Feature extraction uses three techniques: a gray-level co-occurrence matrix, a bag of words, and an intensity histogram. The accuracy of this approach was 91.28%. Over the past few decades, researchers have extensively employed various deep-learning approaches for the detection and classification of brain tumors. Sajid et al.[25] proposed a fully automated hybrid method using deep learning to detect and segment brain tumors on MRIs. Using the BRATS2013 dataset, they achieved a Dice score of 86%, a sensitivity of 86%, and a specificity of 91%. Saxena et al.[26] employed ResNet-50, Inception V3, VGG-16, and transfer learning techniques for image

classification, with ResNet-50 outperforming the others with 95% accuracy. In their work[27], with the help of various convolutional neural network (CNN) models such as Inception V3, GoogLeNet, ResNet-50, AlexNet, and DenseNet-201, Çinar, and Yildirim achieved impressive accuracy in every instance, and classification of brain MRIs using a modified version of the AlexNet architecture, as demonstrated by Khwaldeh et al.[28], achieved a 91% success rate. An architecture that combines wavelet-based gray-level co-occurrence matrices (GLCM) to generate feature matrices was presented by Preethi and Aishwarya[29]. Their deep neural network classifier could detect and classify brain MRI scans with a 92% success rate. For brain tumor classification, Hemanth et al.[30] presented a modified deep convolutional neural network (DCNN) that showed remarkable accuracy in model performance. Khan et al.[31] presented an automated multimodal classification method that uses feature extraction from two pre-supervised convolutional neural network (CNN) models, namely VGG16 and VGG19. Validating their model with the BRATS2018 dataset, they achieved an accuracy of approximately 97.80%. First, using contrast optimization and nonlinear techniques, Guan et al.[32] improved the visual quality of input images. The next step was to use segmentation and clustering methods to pinpoint the exact locations of tumors. Subsequently, we use the associated input image and score the locations to feed EfficientNet for feature extraction. Further optimization of these locations was performed to enhance the detection performance. Finally, the aligned locations were used to identify tumor classes and their locations. This study achieved 98.04% accuracy with five-fold cross-validation of the T1W-CE MRI dataset. One limitation of this study is that training many networks increases computational cost.

Badža et al.[33] employed a Convolutional Neural Network (CNN) consisting of 22 layers to categorize tumors in the T1W-CE MRI dataset into three groups: meningioma, glioma, and pituitary. The researchers performed ten-fold cross-validation on both the enhanced and original image databases, considering each subject and recording separately. The best level of precision, achieved by performing ten-fold cross-validation on individual records using an enhanced dataset, was 96.56% on the 3064 T1W-CE MRI dataset. Deepak et al.[34] utilized deep learning and machine learning techniques by making modifications to a pre-trained GoogleNet model using the Adam optimizer. The system accuracy improved when the SVM or KNN was employed instead of the classification layer within the transfer learning model. By employing five-fold cross-validation on the T1W-CE MRI dataset, the researchers attained accuracies of 92.3, 97.8, and 98% for the GoogleNet, SVM, and KNN models, respectively. This study has significant limitations, despite its ability to effectively classify the three different forms of brain tumors. Initially, the transfer-learned model exhibited subpar performance when used as a standalone classifier. Furthermore, notable misclassification was observed in samples belonging to the meningioma class.

The regularized extreme learning machine (RELM), introduced by Gumaei et al., is a hybrid feature-extraction method[35]. Improving the contrast of brain edges was the first step in pre-processing brain images using min-max normalization. The next step was to extract brain tumor features using a PCA-NGIST hybrid method, which combined PCA with a normalized GIST descriptor to find important features. Subsequently, the T1W-CE MRI dataset was used to train the RELM to classify various brain tumor types, with a five-fold cross-validation accuracy of 94.233%.

Numerous studies have focused on automating the classification of brain cancers using magnetic resonance imaging (MRI). The essential steps in the machine learning process for this purpose include data cleaning, feature extraction, and feature selection, followed by the construction of an ML model based on labeled samples. In[36], a neural network-based approach was presented for classifying MR brain images as normal or abnormal. This method involves extracting features using wavelet transform, followed by dimensionality reduction using PCA. The reduced features were input into a back-propagation NN utilizing a scaled conjugate gradient to determine the optimal weights, achieving 100% classification accuracy on 66 images comprising 18 normal and 48 abnormal cases. Arakeri and Reddy[37] proposed an automated computer-aided diagnosis technique using ensemble classifiers to classify brain MRI scans in the presence or absence of cancer. Furthermore, a new method for MRI brain tumor classification using improved structural descriptors was proposed in[38] along with a hybrid kernel-support vector machine using a classifier. To refine image classification and enhance texture feature extraction using statistical parameters, they employed a gray-level co-occurrence matrix and histograms. The proposed hybrid kernel SVM classifier, which integrates different kernels, achieves 93% accuracy, specifically for axial T1 brain MRI images.

In[39], a hybrid system comprising two machine-learning techniques was recommended for brain tumor classification. This study considered 70 brain MR images, including 60 abnormal and 10 normal cases. Features were extracted from the images using discrete wavelet transform, and the total number of features was reduced using principal component analysis. After feature extraction, feed-forward backpropagation, artificial neural networks, and k-nearest neighbors were applied separately to the reduced features. FP-ANN covers the backpropagation learning technique for updating the weights. Using the KNN and FP-ANN, this technique achieved accuracies of 97% and 98%, respectively.

Khazaee et al.[40] introduced an innovative AI diagnosis model, EfficientNetB0. Operating on the BRATS-2019 dataset, this model leveraged convolutional neural networks (CNNs) and transfer learning to classify and rate glioma images, achieving an impressive accuracy of 98.8%. Another study[41] enhanced the accuracy of germinoma identification in the basal ganglia by implementing transfer learning and a pre-trained ResNet18 model. In a retrospective analysis involving the manual segmentation of brain tumors in 73 patients with basal glioma using T1 and T2 data, a tumor classification model was developed using a 2D convolutional network and transfer learning with the T1 sequence. Through a five-fold cross-validation, this model achieved an average AUC of 88%. Additionally, an approach to optimize CNN hyperparameters using Bayesian optimization was proposed[42]. The study evaluated 3064 T1 images representing three types of brain cancers: glioma, pituitary, and meningioma. Five well-known deep-pretrained models were compared with a transfer-learning-enhanced CNN, which demonstrated a remarkable validation accuracy of 98.70% after Bayesian optimization. Alanazi

et al.[43] devised a generated transfer deep learning model for detecting meningiomas, pituitary adenomas, and gliomas in early brain cancer detection. By employing transfer learning to adjust the neuronal weights, this method produced a transfer-learned model with an accuracy rate of 95.75%. The model classifies brain MRI images into tumor subclasses using a 22-layer isolated CNN model.

In the realm of brain tumor classification, Rizwan et al. proposed an innovative approach that utilized a Gaussian CNN on two distinct datasets[44]. The primary objective of the initial dataset, comprising 233 cases and 3064 T1-enhanced images, was to categorize lesions into pituitary, glioma, and meningioma classes. The second dataset, with 73 cases and 516 images, aimed to differentiate between three glioma classes (II, III, and IV). Remarkably, both datasets exhibited high accuracy rates of 99.8% and 97.14%, respectively, as achieved using the proposed method. Another study[45,46] proposed a seven-layer CNN for sorting brain MR images into three groups, employing separable convolution to reduce computational time. The final layers were modified using various pre-trained convolutional neural networks (CNNs): GoogleNet, Alexnet, Resnet50, Resnet101, VGG-16, VGG-19, InceptionResNetV2, and Inceptionv3. AlexNet, implemented with transfer learning on a 60:40 split dataset, demonstrated superior speed and accuracy, achieving accuracies of 100%, 94%, and 95.92% across three datasets. The approach in[47] utilized three distinct CNN designs (VGGNet, AlexNet, and GoogleNet) to classify meningiomas, gliomas, and pituitary tumors. By employing data augmentation on MRI slices, transfer learning methods such as fine-tuning and freezing have been investigated to enhance generalization, increase dataset samples, and mitigate overfitting. The results revealed that the fine-tuned VGG16 architecture achieved the highest accuracy of 98.69%. To enhance brain tumor segmentation and classification accuracy[48], introduced a hybrid optimization method that incorporated CNN features. In complex neural networks, residual connections are employed to mitigate the problem of vanishing gradients. The residual approach, as described in[61], has been implemented for the classification of glioma tumors, resulting in enhanced accuracy. Additionally, the attention mechanism, a recent advancement in neural network architecture, has been applied in[62]. This approach specifically improves the focus on tumor regions, thereby facilitating more efficient detection.

Proposed system

This proposed system introduces advancements in feature extraction. Two models, MobileNetV3 and EfficientNetB7, are employed to extract relevant features related to brain tumor images. Both networks undergo training on brain tumor images, extracting features based on their respective architectures. The extracted feature maps from both networks contain crucial information for distinguishing between different types of brain tumors. These feature maps have distinct levels: intermediate-level features are extracted from the middle of the architecture, while final-level feature maps are derived from the last layer of the network. In total, four feature maps are obtained—two from MobileNet and two from EfficientNet. Following the extraction of feature maps, an attention mechanism is applied at both intermediate and final levels. This mechanism dynamically modulates the significance of individual features, allowing the model to focus on specific regions crucial for global-level feature extraction. The integration of attention mechanisms enhances the model's ability to accurately identify varied feature patterns within brain tumor images. In the final stage, all attention feature maps are combined through a simple averaging function to generate the global-level feature map. This comprehensive feature set incorporates information from various levels, including the model, local, and global levels. This significantly improves the accuracy of the classification process. The enriched feature set is then fed into the SoftMax classifier, enabling the model to effectively identify and classify different tumor classes. Overall, this approach represents a multifaceted feature extraction strategy that leverages the strengths of both MobileNetV3 and EfficientNetB7 architectures, enhancing the model's ability to differentiate complicated patterns in brain tumor images for more accurate classification. Figure 1 shows the overall proposed architecture.

$$F = [Mi.Mf, Ei, Ef] \tag{1}$$

$$Attention\ Weights\ = [Mai, Maf, Eai, Eaf] \tag{2}$$

$$Ensemble\ Attention = \frac{(Mi * Mai + Mf * Maf + Ei * Eai + Ef + Eaf)}{4} \tag{3}$$

Mi, *Mf* represents the intermediate and final feature map of MobileNetv3, *Mai*, *Maf* corresponding attentions.

Ei, *Ef* represents the intermediate and final feature map of EfficientNetB7, *Eai*, *Eaf* corresponding attentions, *F* is the all features.

Dataset and preprocessing

The primary goal of preprocessing is to improve image quality, thereby enhancing the accuracy of the classification process. The specific steps of each phase are detailed below. The resizing and data augmentation phases include gathering images from all four classes. These images underwent augmentation, which involved horizontal and vertical flipping, rotation, combined horizontal and vertical transformations, and power-law transformations, with c = 1 and gamma = 0.52. This expanded the dataset and provided a larger number of images for fine-tuning the proposed algorithm.

This study utilized two datasets first one is from Figshare which is available in Kaggle and another from BraTs 2019 dataset, The Figshare dataset has three types of tumor classes, The Brats contains MRI scans with four different contrasts T1, T1 contrast-enhanced, T2, and FLAIR[60]. Among the various MRI contrasts available, T1 contrast-enhanced (T1ce) is commonly preferred for single-contrast tumor classification[12]. Therefore, this paper focused on T1ce images from the BraTS 2019 dataset, specifically using 332 subjects, 259 volumes from Glioblastoma high-grade glioma (HGG), and 73 volumes from low-grade glioma (LGG). The healthy sample

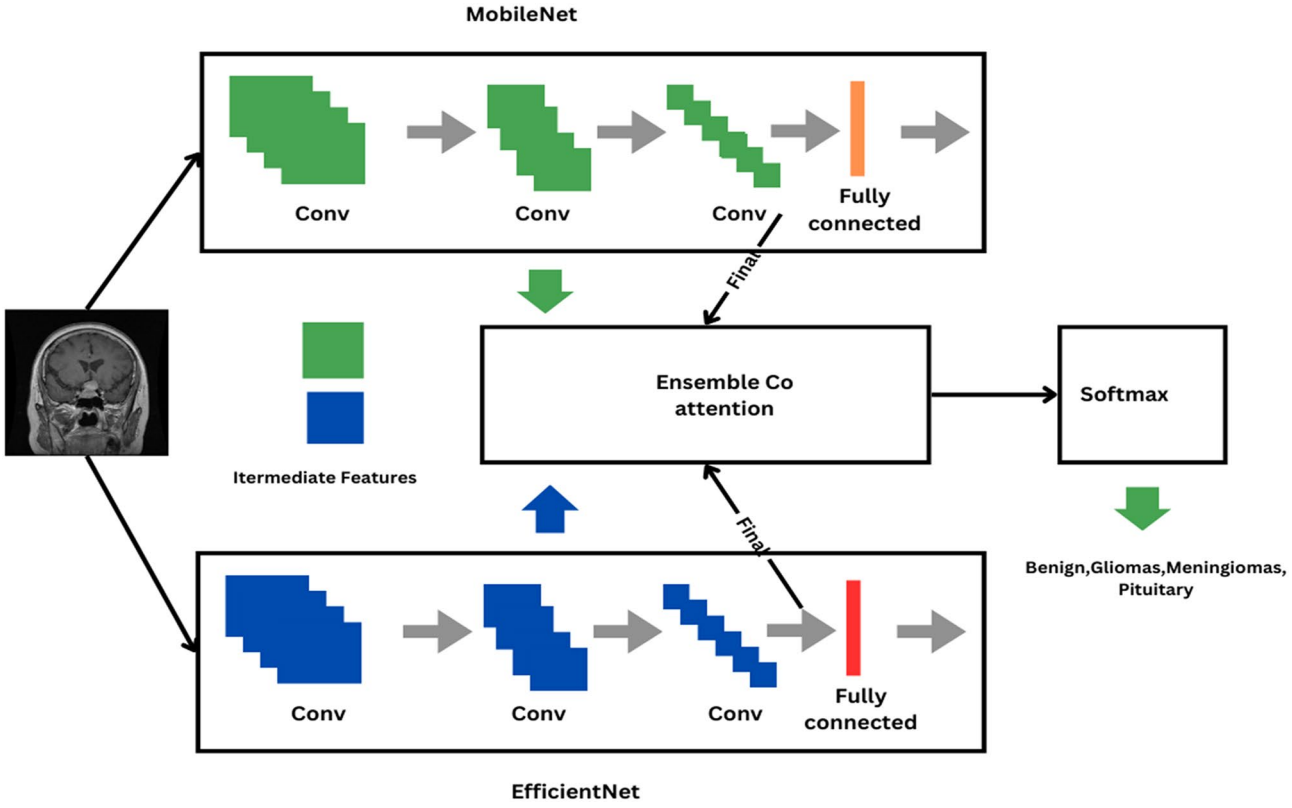

Fig. 1. Proposed architecture.

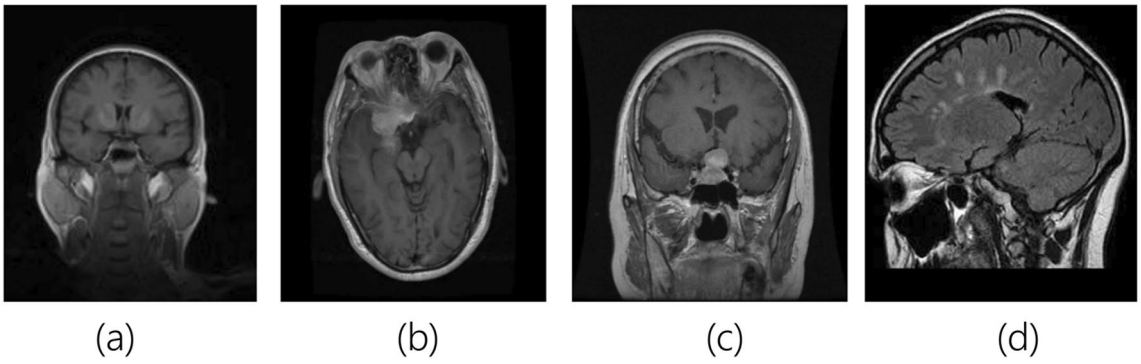

Fig. 2. Sample brain tumor images – Figshare Dataset. (**a**) No tumour, (**b**) gliomas, (**c**) meningiomas, (**d**) pituitary.

was taken from the first dataset. Sample images of the figshare dataset are shown in Fig. 2. BraTs 2019 dataset sample images are displayed in Fig. 3.

MobilenetV3

MobileNetV3 is chosen as the base model due to its lightweight architecture, making it particularly well-suited for resource-constrained environments without compromising on performance. This model incorporates depthwise separable convolutions and efficient building blocks, allowing it to efficiently extract meaningful features from images.

In the process of fine-tuning, the pre-trained MobileNetV3 is utilized to leverage the knowledge combined during training. This application of transfer learning enables the model to adeptly generalize to the individual features essential in brain tumor images. By connecting pre-trained weights, the network optimally capitalizes on its essential capacity to discriminate relevant features useful for brain tumor classification.

The MobileNetV3-Large pre-trained model, illustrated in Fig. 4, was used in the method. Adjustments were made following the conventional method for refining the MobileNetV3 model to extract the relevant

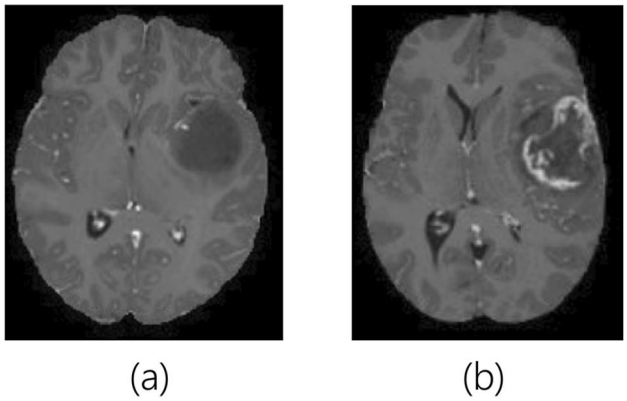

Fig. 3. Sample brain tumor images –BraTs 2019. (**a**) LGG and (**b**) HGG.

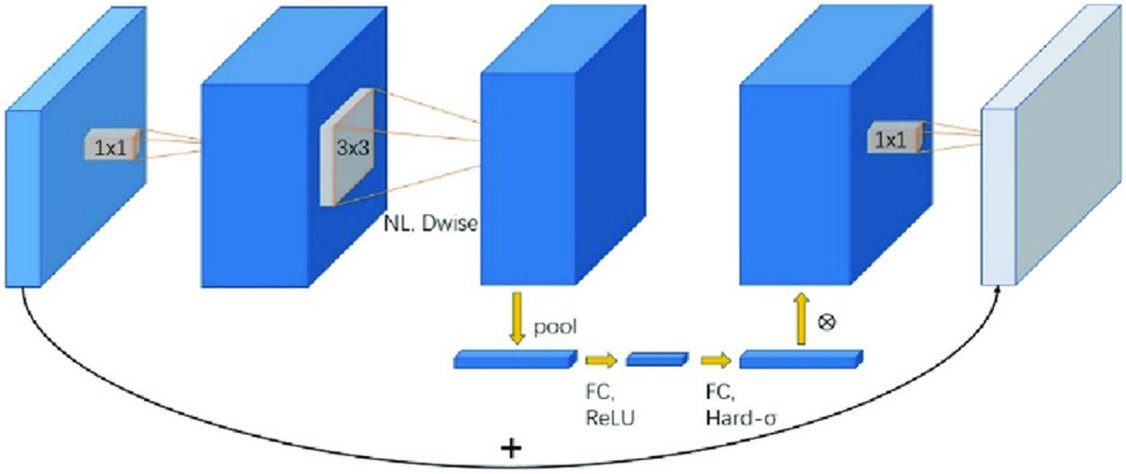

Fig. 4. MobilenetV3 Core.

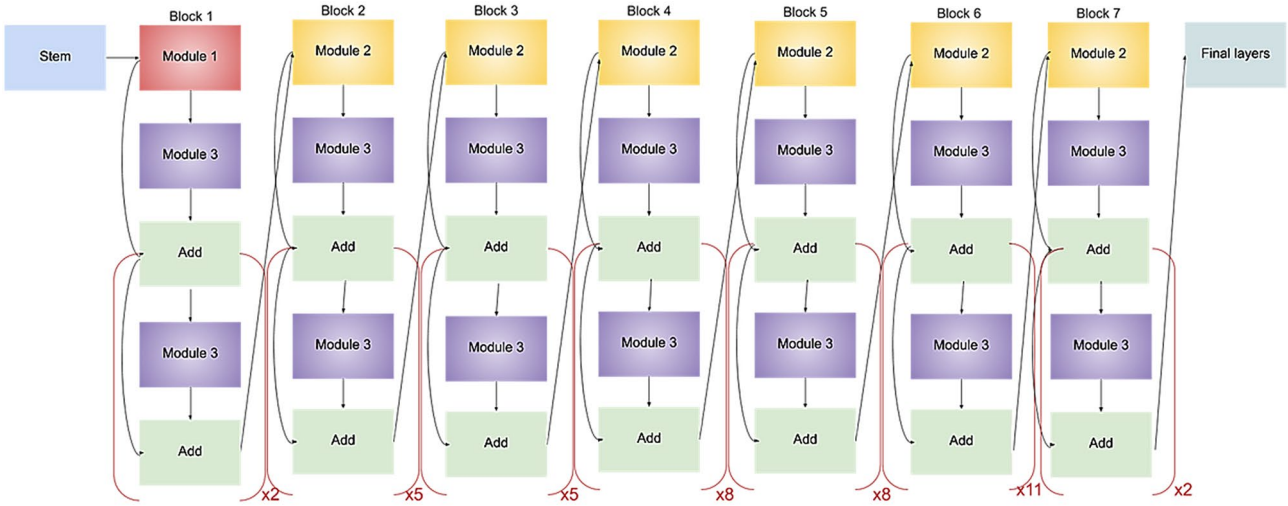

Fig. 5. EfficientNet-B7.

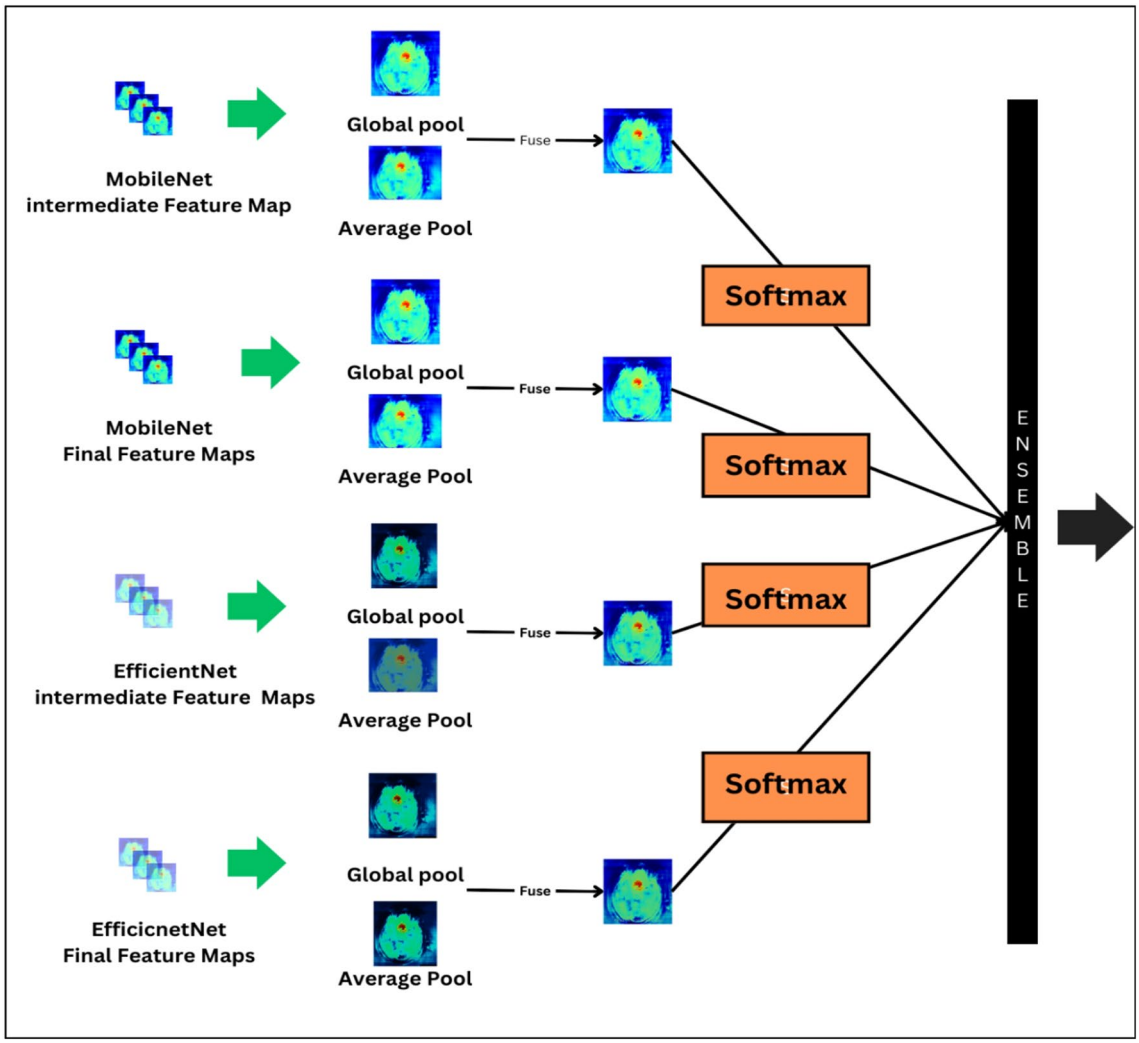

Fig. 6. Ensemble Attention mechanism.

image features. The initial step involved replacing the top two output layers of the image-classification-focused MobileNet model with a 1 × 1 point-wise convolution, facilitating the extraction of features from images. This convolution, serving as a multilayer perceptron, can incorporate various nonlinear operations for image classification or dimensionality reduction. Additional 1 × 1 point-wise convolutions were then added atop the model to fine-tune the weights for different datasets based on the classification task. Following the fine-tuning process, the output from the 1 × 1 point-wise convolution used for feature extraction was compressed, resulting in 128-pixel image features for each image in the dataset. Finally, the extracted image features were fed into the attention mechanism.

The MobileNetV3 model is involved in the attention mechanism. The attention mechanism was applied to both the intermediate features and the final layer features of MobilenetV3. In the attention mechanism, both intermediate and final features undergo max pooling and average pooling operations. Subsequently, the results are fused, and Softmax activation is applied.

Efficient net

The EfficientNet model is also a good classification model, This model employs a simple but effective method known as compound coefficient. Instead of arbitrarily increasing the width, depth, or resolution, compound scaling uses a predetermined set of scaling coefficients to scale each dimension uniformly.

The architecture of EfficientNet consists of a baseline network, denoted EfficientNet-B0, which serves as the starting point for the family of models created through a compound scaling method. This method involves simultaneously adjusting three key dimensions: width (φ), depth (α), and resolution (β). The scaled network dimensions were determined by multiplying the base width, depth, and resolution by their respective scaling coefficients. EfficientNet utilizes a depth-wise separable convolutional block as its basic building block, which consists of depth-wise convolution followed by point-wise convolution. This block helps reduce the computational complexity while maintaining expressive power. Compound scaling enables the creation of various EfficientNet models, such as B0 to B7, each with a progressively increased capacity. This architecture balances model size

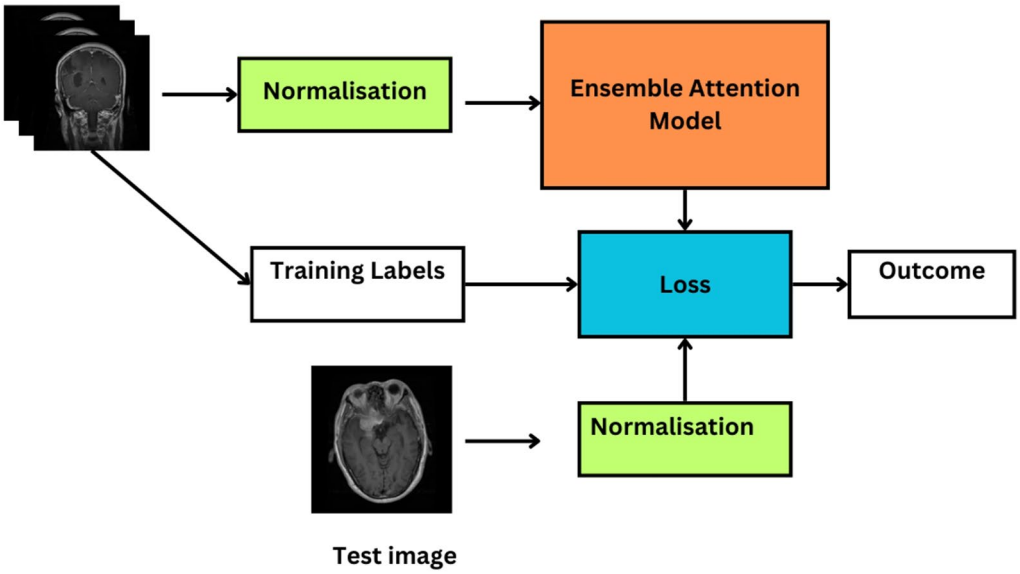

Fig. 7. Experimental Setup.

Parameter	Value
Epoch	100 randomly 5 times
Batch size	32
Initial_lr, Maximum_lr	1e-6, 4e-5
Loss	Cross entropy
Evaluation	Accuracy

Table 1. Training parameters.

and performance, making it efficient for a wide range of applications, particularly in scenarios with limited computational resources.

We implemented the EfficientNetB7 model and introduced an attention mechanism, applying it to both intermediate and final layer features. In this attention mechanism, both the intermediate and final features undergo max pooling and average pooling operations, followed by fusion. The fused data were then directly fed into the SoftMax activation. This approach enhances the capability of the model to capture complex patterns and relationships within the data before making predictions. Figure 5 shows the EfficientNet-B0 model.

Ensemble attention mechanism

Attention mechanisms in image classification play a pivotal role in enhancing the interpretability and performance of neural networks by enabling them to focus selectively on relevant regions within an image. In our approach, we employed ensemble attention to further improve overall classification accuracy. The attention mechanism was applied at spatial levels, involving intermediate and final feature maps. The process begins with the extraction of these feature maps, followed by the application of average and global pooling. The pooled feature maps are then fused to create a comprehensive representation. Subsequently, SoftMax was applied to generate a probability map based on the fused outcome, which was multiplied by the original feature map to obtain the focused features. This attention mechanism is individually applied to both the MobileNetV3 and EfficientNetB7 models, resulting in four attention outcomes. To make a collective decision and capitalize on the strengths of both models, we employ an ensemble strategy. The ensemble can be achieved by averaging the individual attention outcomes. This strategic ensemble approach aims to enhance the robustness and generalization of the model by combining focused features from both MobileNetV3 and EfficientNetB7 at different levels. The collaborative integration of attention mechanisms and ensemble strategies contributes to a more powerful and accurate brain tumor classification model, as shown in Fig. 6.

An ensemble here is used to combine the focused feature outcomes from multiple levels to improve the overall performance. One common way to ensemble models is to average their outcomes. Here's the equation for the ensemble using simple averaging.

Let M be the number of models, and let $P(i, j)$ The predicted probability for class i from the $j-th$ feature model

For a classification task, the ensemble prediction $y\prime$ for class i can be calculated as

$$y' = \frac{1}{M}\sum_{j=1}^{M} P(i,j) \tag{4}$$

This equation calculates the average probability for class i across all the feature map models. The class with the average probability is given to the next processing

Input: Training images are represented by Tim using the following inputs: validation image data (V_d), learning rate (L_r), optimizer (O), and the specific number of class labels (c_L).

Output- MobileNet feature map, EfficientNet feature map, loss, and accuracy,

Set the learning Rate L_r as low

Step1: For Z= 1 to the total no of images Tim

Input Image: X

CNN-MobileNetV3,EfficientNetB0

Step2: Get intermediate and Final feature map (X)

Do average pooling (Pa) and global pooling (Pg)

Feature map= $Pa+Pg$

Step3: Apply SoftMax

Step4: Do Ensemble Attention

$E = \frac{F1+F2+F3+F4}{4}$

Step5: Softmax Classifier (Z):

Z=SoftMax(E)

Get the output of feature map, accuracy, and loss values,

Algorithm 1. Ensemble Attention Algorithm

This algorithm outlines a comprehensive approach for training a classification model. Utilizing a combination of MobileNetV3 and EfficientNetB7 architectures, the algorithm employs the Adam optimizer to reduce the cross-entropy loss during backpropagation. With a specified low learning rate, each image in the training dataset underwent feature extraction through both the MobileNetV3 and EfficientNetB0 networks, resulting in intermediate and final feature maps. The application of average pooling, global pooling, and subsequent pooling result fusion contribute to the generation of a feature map. Following SoftMax activation, an ensemble mechanism combines the outputs from MobileNetV3 and EfficientNetB7 through attention. The SoftMax classifier was then applied, resulting in the output of the model for each image. The algorithm provides training data feature maps, loss metrics, and accuracy metrics, offering a comprehensive framework for efficient and accurate classification.

Training options

After completing 100 epochs of fine-tuning, five randomly initialized runs were performed. The model with the highest classification accuracy was selected for each dataset. During fine-tuning, a batch size of 32 was employed, and the Adam optimizer was utilized with a learning rate set to 1 × 10^−4. Data augmentation was implemented during the preprocessing phase to address overfitting and enhance model generalization. In addition to the original image resizing, several data augmentation techniques, including random cropping, random horizontal flip, color jitter, and random vertical flip, were applied to achieve a final image shape of 224 × 224.

Loss and optimizer

For the multiclass classification task, the Cross-Entropy Loss is computed as follows:

$$L(yi, yi\prime) = -\sum_{i=1}^{C}(yi * logyi' \tag{5}$$

where L denotes the cross-entropy loss. C is the number of classes. yi is the true probability distribution (one-hot encoded vector) for class i. yi' is the predicted probability for class i.

The loss function is often used in neural network training to convert the raw output scores into probability distributions across classes. Cross-entropy loss measures the difference between the predicted and true distributions to assign higher probabilities to correct classes. This is achieved through optimization algorithms, such as Adam, which dynamically adjust the learning rates for each parameter, making it suitable for complex neural network models.

The equation for the Adam optimizer update rule, combining the exponential moving averages of gradients (mt) and squared gradients (vt^) with bias correction and performing parameter updates, is given by

$$\theta\, t+1 = \theta\, t - v^t + \epsilon\alpha \cdot m^t \tag{6}$$

where:

$\theta\, t$ represents the model parameters at the time step t, α is the learning rate,ϵ is a small constant added to the denominator for numerical stability, m^t is the exponential moving average of the gradient at time t, v^t is the exponential moving average of the squared gradient at the time t.The Adam optimizer is widely used in training deep neural networks due to its adaptive learning rate capabilities and overall effectiveness

Results and discussion

To examine the outcomes, a quantitative analysis was conducted to systematically evaluate the models with attention. The primary focus was to understand how attention mechanisms affect system performance at different levels and assess the effectiveness of different ensemble techniques. Also investigated the influence of attention mechanism, both individually and in grouping. A detailed scrutiny of these models was performed to comprehend their contributions at different stages, covering both the intermediate and final features.

Data augmentation

We made our dataset larger and more varied by changing the images slightly. We rotated, translated, and resized them. This helps our model learn to better recognize brain tumors, even when they occur in different sizes.

Figure 7 illustrates the outcomes of our experiments, providing a complete overview of the setup for both training and testing data for brain tumor classification. The system performance was evaluated by examining the classification metrics. True positive (TP) denotes instances in which the system accurately identifies a brain tumor, whereas false positive (FP) signifies cases in which it incorrectly identifies a tumor. True negative (TN) represents the number of correct identifications in the absence of a brain tumor, and false negatives (FN) correspond to instances where the system fails to recognize the present tumor. These parameters were expressed mathematically to quantify and analyze the accuracy of the system for classifying brain tumors. The formulas given by Eqs. (7–10) were used to determine the F1 Score, Precision, Accuracy, and Recall.

$$\text{Accuracy} = \frac{\text{Tp} + \text{Tn}}{(\text{Tp} + \text{Tn} + \text{Fp} + \text{Fn})} \tag{7}$$

$$\text{Recall} = \frac{\text{Tp}}{\text{Tp} + \text{Fn}} \tag{8}$$

$$\text{Precision} = \frac{\text{Tp}}{\text{Tp} + \text{Fp}} \tag{9}$$

$$Accuracy = \frac{2^{*}\,(\text{Precision} + \text{Recall})}{(\text{Precision} + \text{Recall})} \tag{10}$$

The confusion matrix is a performance measurement tool that is commonly used in classification tasks. Each matrix allowed for a detailed examination of the model's performance by representing the distribution of predicted and actual class labels. Figures 8 and 9, and 10 provide a visual representation of the confusion matrices associated with separate models and proposed system.

The model for brain tumor detection used a robust training strategy, with 100 epochs repeated five times for stability and pattern capture. A batch size of 32 and a dynamic learning rate schedule enhanced the efficiency. The cross-entropy loss function measures classification dissimilarity. The performance was evaluated based on the accuracy. The training parameters are presented in Table 1.

In a comparative analysis of the brain tumor classification models, including MobileNetV3, EfficientNetB7, MobileNetV3-Attention, EfficientNetB7-Attention, and our proposed method, our proposed method achieved the highest possible F1 score, recall, accuracy, and precision. The proposed method proved to be highly effective in classifying brain tumors, as evidenced by its superior performance across various metrics. The incorporation of attention mechanisms in MobileNet and EfficientNet variants, aimed at enhancing feature extraction, obtained improved results compared with the base architectures. Our proposed method exhibited a comprehensive advancement against these models, its Tabulated in Table 2.

In the comparison of MobileNetV3-Attention, EfficientNetB7-Attention, and our proposed model, the performance metrics were considered with a focus on accuracy and loss. Our proposed model demonstrated superior validation accuracy, indicating its ability to correctly classify brain tumors during the evaluation phase. The validation accuracy was notably higher than that of both MobileNetV3-Attention and EfficientNetB7-Attention. High validation accuracy suggests that our model achieved a greater proportion of correct predictions on unseen data, signifying its effectiveness in generalizing new cases. Simultaneously, the loss function was analyzed to assess the convergence and optimization of the models during training. Our proposed model exhibited a lower loss than MobileNetV3-Attention and EfficientNetB7-Attention. A lower loss signifies that the model predictions were closer to the actual values, indicating effective learning and improved convergence during the training process. Throughout the training process, our proposed model demonstrated consistent improvements in both accuracy and loss. The training curves for accuracy showed an upward trend, reaching a high validation accuracy, whereas the loss curves exhibited a consistent decrease, confirming the model's ability to minimize prediction errors over successive epochs. This steady improvement in accuracy and reduction in loss highlights the efficacy of our proposed model in learning and extracting relevant features for accurate brain tumor classification. The superior performance in both accuracy and loss metrics underscores the effectiveness of our model in comparison with MobileNetV3-Attention and EfficientNetB7-Attention throughout the training process. The comparison between the model and MobileNetV3-Attention and EfficientNetB7-Attention indicates better performance in terms of accuracy and loss. This is clearly illustrated in Fig. 11 , 12, 13. 14. 15. 16.

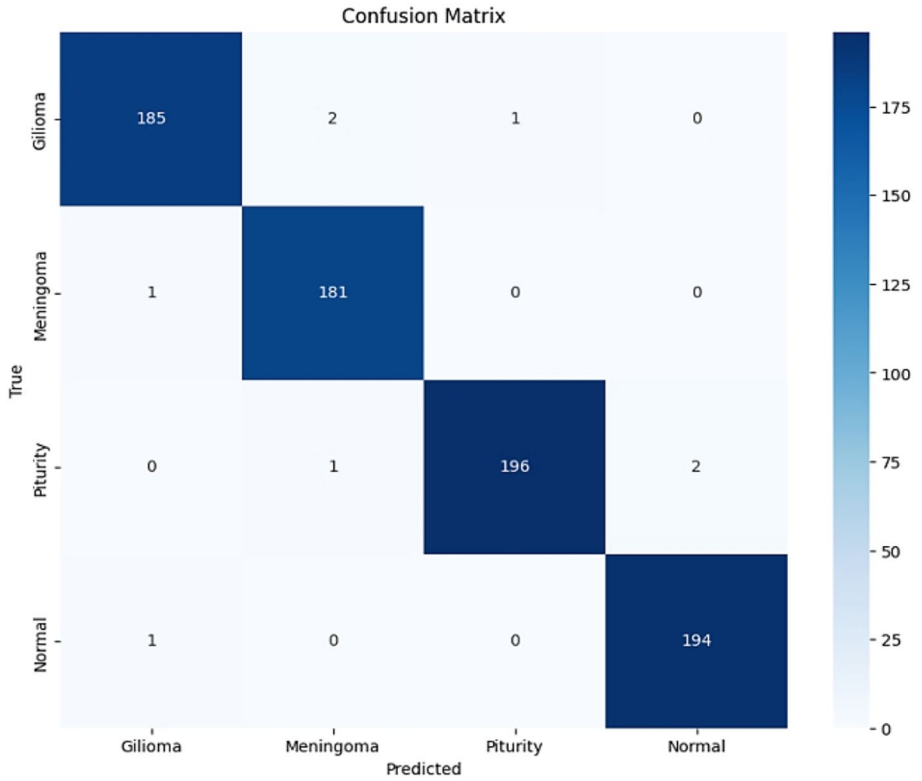

Fig. 8. Confusion matrix- Attention MobileNetV3.

Table 3 illustrates the various ensemble techniques and their respective performances, showing their comparative effectiveness. Notably, both Majority Voting and Weighted Averaging exhibited lower results compared with simple averaging. The straightforward averaging approach proved to be more beneficial in leveraging concentrated features, resulting in higher performance.

Figure 17 shows the performances of the different attention models. The specified models, namely 'MobileNetV3-Attn-Inter' means it has only intermediate feature map attention, 'MobileNetV3-Attn-Final' has the final feature map with attention 'MobileNetV3-Attn-Fuse,' it has both intermediate and final feature map, and proposed, likewise for EfficientNetB7 are evaluated based on precision, F1 score, recall, metrics. Precision, which indicates how well positive predictions turn out, is crucial for minimizing the number of false positives. Recall that the model's ability to capture all actual positive instances becomes significant when reducing false negatives is prioritized. The F1 score offers a balanced measure that takes both false positives and false negatives into account; it is the harmonic mean of recall and precision. The final level feature map gets better values compared to the intermediate level. Over all the proposed method obtained good results compared to others.

.

Table 4 presents a comprehensive evaluation of various EfficientNet models, ranging from B0 to B7, augmented with the Ensemble Attention mechanism, for the critical task of brain tumor detection. The table illustrates a discernible upward trajectory in the classification accuracy as the complexity of the EfficientNet models increases. Starting at 95.1% accuracy for EfficientNetB0 with Ensemble Attention, the results steadily increased, reaching a notable accuracy of 97.91% for EfficientNetB7 with Ensemble Attention. This progression underscores the effectiveness of deeper and more intricate models for capturing nuanced patterns within brain images. The consistent integration of the Ensemble Attention mechanism across all variants demonstrates its positive impact on enhancing classification performance. However, it is essential to acknowledge the inherent trade-off between accuracy and computational complexity. Although larger models, such as EfficientNetB7, exhibit superior accuracy, their deployment in real-time applications may necessitate careful consideration of computational resources. Overall, the study not only highlights the success of the proposed Ensemble Attention model in improving accuracy but also provides valuable insights for selecting an optimal EfficientNet variant based on the desired balance between performance and efficiency in brain tumor detection systems.

Table 5 evaluates the efficacy of different MobileNet architectures in the context of brain tumor detection, employing the Ensemble Attention (Ensemble Attn) mechanism to enhance classification accuracy. The summarized results revealed a progressive improvement in accuracy across MobileNetV1, MobileNetV2, and MobileNetV3, reaching 94.9%, 96.2%, and 97.1%, respectively. The consistent application of Ensemble Attention is instrumental in refining the feature extraction, emphasizing its adaptability across diverse MobileNet versions. MobileNetV3, when coupled with Ensemble Attention, has emerged as a noteworthy candidate for brain tumor detection, showing a competitive accuracy comparable to EfficientNet variants. The findings provide valuable insights into the interplay between MobileNet architectures, attention mechanisms, and classification

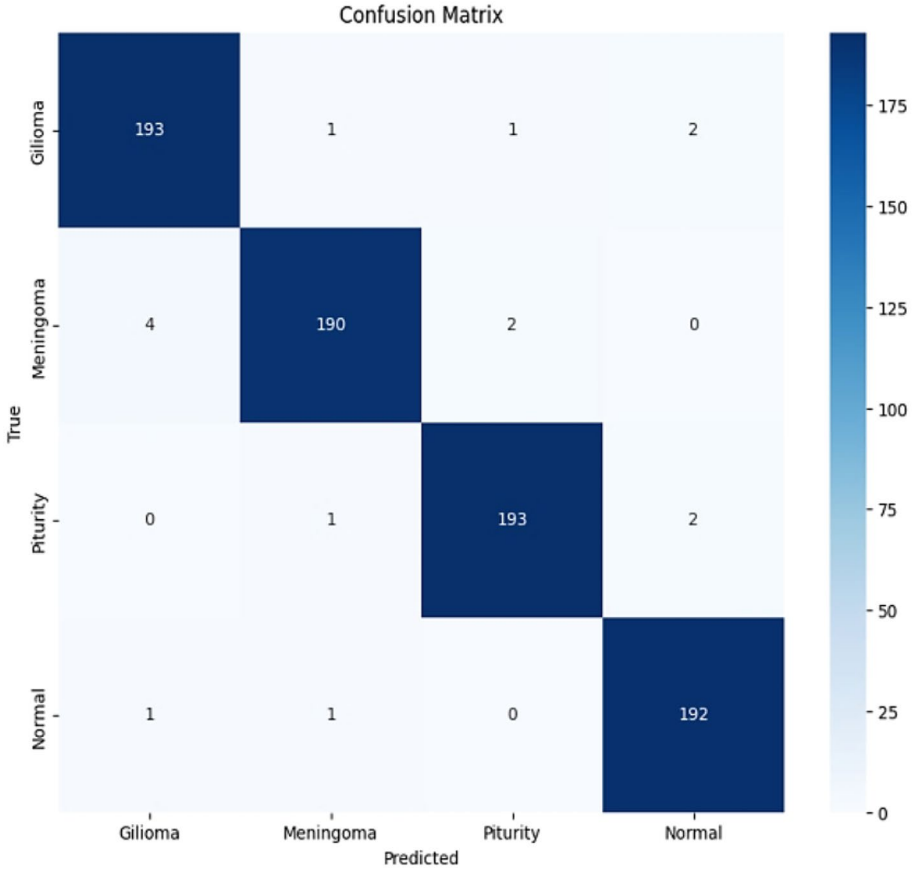

Fig. 9. Attention EfficientNetB7- Confusion Matrix.

performance, aiding the informed selection of models tailored to specific computational and accuracy requirements in healthcare applications.

In the evaluation of MobileNetV3-Attention, EfficientNetB7-Attention, and our proposed model, the Receiver Operating Characteristic (ROC) curve served as a crucial performance metric, as shown in Fig. 18. The area under the ROC curve (AUC-ROC), a quantitative measure of the model's ability to discriminate between classes, was notably higher for our proposed model, indicating its enhanced capability to distinguish between tumor and non-tumor instances. The higher AUC-ROC underscores the improved overall performance and discriminative power of our proposed model in comparison to the attention-enhanced variants. Throughout the evaluation, the ROC curve for our proposed model consistently demonstrated better trade-offs between sensitivity and specificity, confirming the effectiveness in brain tumor classification.

The provided accuracy percentages represent the performance of different models or configurations in a classification task tabulated in Table 6. Firstly, combinations of MobileNetV3 with attention and EfficientNetE7 models were evaluated. The MobileNetV3Attn + EfficientNetB7 combination achieved an accuracy of 95.8%. By incorporating attention mechanisms in the intermediate layers (MobileNetV3Attn_Inter) and final layers (MobileNetV3Attn_Final) of MobileNetV3 with EfficientNetB7, the accuracies improved to 96.9% and 96.7%, respectively. Similarly, when EfficientNetE7 was combined with MobileNetV3, the EfficientNetAttnB7 + MobileNetV3 model reached an accuracy of 96.2%. Enhanced results were observed by incorporating attention in the intermediate (EfficientNetB7Attn_Inter) and final (EfficientNetB7Attn_Final) layers of EfficientNetB7 with MobileNetV3, achieving accuracies of 96.9% and 97.1%, respectively. Finally, a proposed model, not explicitly detailed in terms of its architecture, achieved an accuracy of 98.94%. The results collectively demonstrate the impact of attention mechanisms and their placement in improving the classification accuracy, proposed method showing the highest accuracy among the presented models. The experiment was conducted over multiple trials to assess the consistency, and reliability of the system. The resulting standard deviation value of 0.082 indicates strong performance consistency and reliability for the proposed system.

Here in this section, we analyze the performance of the BraTs 2019 dataset in terms of accuracy and the confusion matrix. The adaptive thresholding is done for segmentation before the classification to find the area of interest. Figures 19 and 20 show the loss and accuracy curve of Brats Datasets. In the analysis of the Brats dataset, In Fig. 19, the loss curve provides the training process of the neural network model. Initially, the loss starts at a higher value, reflecting the early stages of training where the model's parameters are initialized randomly. This high loss indicates that the predictions made by the model are significantly different from the actual values of the dataset, highlighting the model's initial lack of accuracy. As training progresses through multiple epochs, the loss

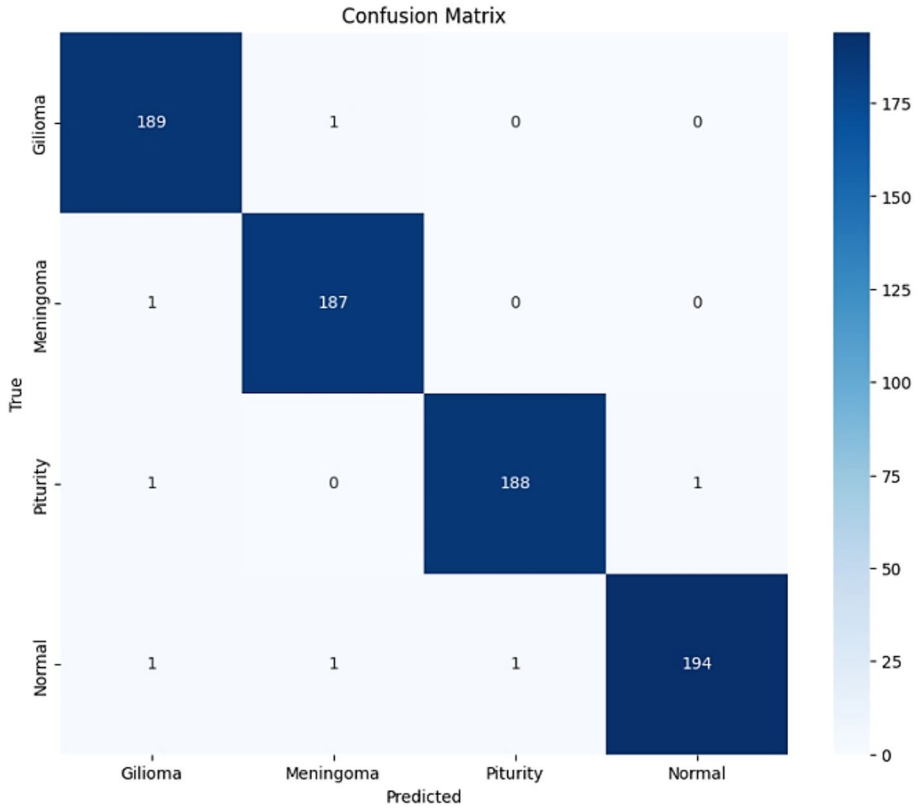

Fig. 10. Proposed Model Confusion Matrix.

Method	Accuracy	Precision	Recall	F1-Score	AUC
MobileNetV3	96.9	96.95	96.95	96.9	96
EfficientNetB7	97.1	97.95	97.95	97.9	96
MobieNetV3-Attention	97.8	97.95	97.95	97.9	96.3
EfficientNetB7-Attention	98.1	98	98.1	98.2	97.2
Proposed (Ensemble Attention)	98.94	98.91	98.93	98.91	98.4

Table 2. Performance comparison for individual model.

gradually decreases. This loss reduction signifies that the model is learning from the dataset: adjusting its internal parameters to better approximate the target outputs. This iterative process of minimizing loss, often through techniques like gradient descent, allows the model to make more accurate predictions over time. Eventually, the loss curve may flatten out, indicating that the model has converged to a stable state. At this stage, the model has captured much of the important patterns in the BraTs dataset,

The confusion matrix in Fig. 21 illustrates the misclassifications among HGG, LGG, and No Tumour categories, most of the samples were detected correctly but there is potential enhancement in classification accuracy needed in the future.

Table 7 shows the different feature-level combinations of MobileNetV3 and EfficientNetB7 architectures. The initial configurations, such as MobileNetV3Attn + EfficientNetB7 achieving 95.2%, highlight the strong baseline capabilities of these models in image recognition tasks. Gradually, configurations like EfficientNetB7Attn_Inter + MobileNetV3 achieve higher accuracies, concluding in EfficientNetB7AttnFinal + MobileNetV3 reaching 97.01%, indicating refinements in attention mechanisms or final adjustments that improve predictive accuracy. Notably, the ensemble model proposal achieves the highest accuracy of 98.28%, underscoring the efficacy of combining multiple model outputs to enhance overall performance and robustness. These findings underscore the iterative improvements and strategic combinations of neural network architectures to achieve superior accuracy in brain tumour classification tasks.

The accuracy scores provided in Table 8. summarize the performance of various models when combined in an ensemble framework. Starting with MobileNetV1 and MobileNetV2 combined with the ensemble, they achieve accuracies of 94.5% and 96.1% respectively, demonstrating their effectiveness as base models in ensemble setups. MobileNetV3 shows further improvement with an accuracy of 96.9%, indicating enhancements in feature extraction and better learning. Moving to EfficientNet models with attention mechanisms (EfficientNetB0

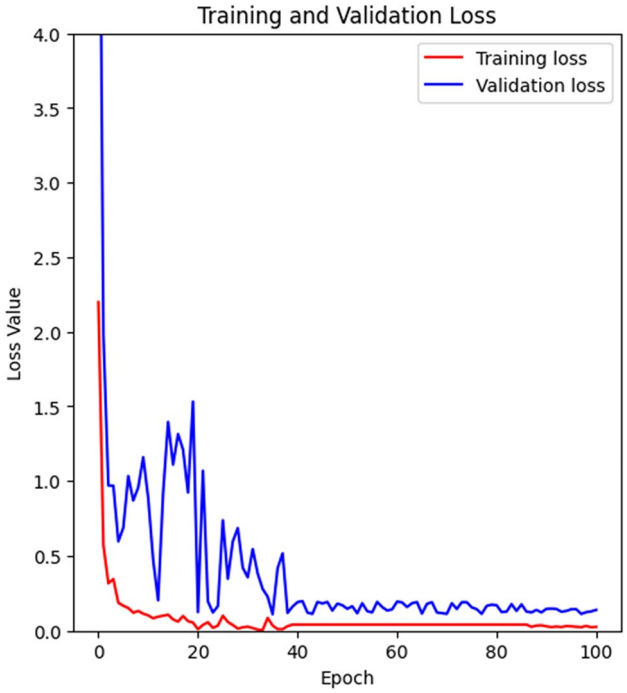

Fig. 11. MobileNetV3-Attention-Loss.

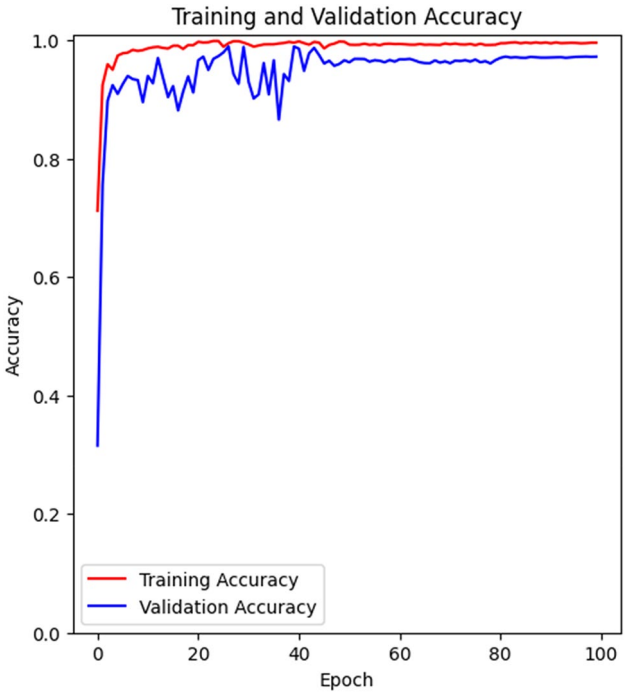

Fig. 12. MobileNetV3- Attention -Accuracy.

to EfficientNetB7), accuracies progressively increase from 94.9 to 97.52%. This progression highlights the performance gains achieved by deeper architectures in combination with ensemble methods. The highest accuracy of 97.52% is attained by EfficientNetB7Attn combined with the ensemble attention. These results underscore the strategic use of ensemble attention techniques to leverage the strengths of individual models and achieve superior accuracy in complex classification scenarios. The standard deviation value is 0.095. it's a little higher compared to the Figshare dataset as both LGG and HGG images look similar.

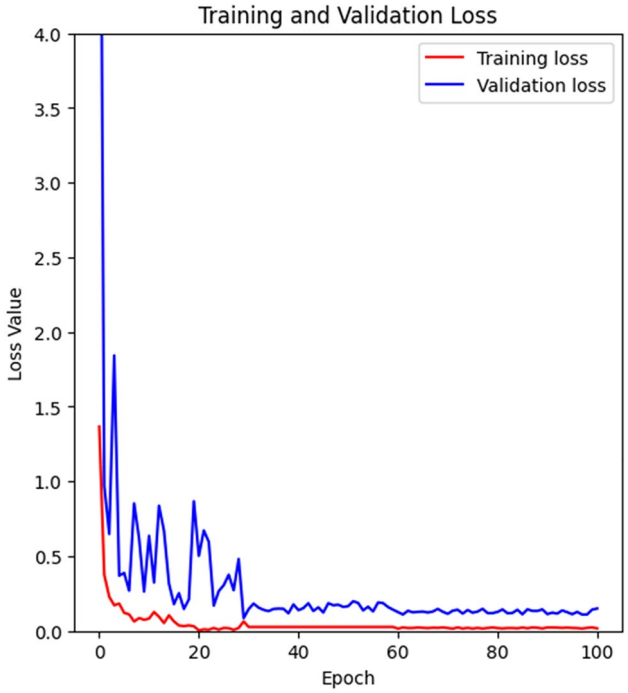

Fig. 13. EfficientNetB7-Attention-Loss.

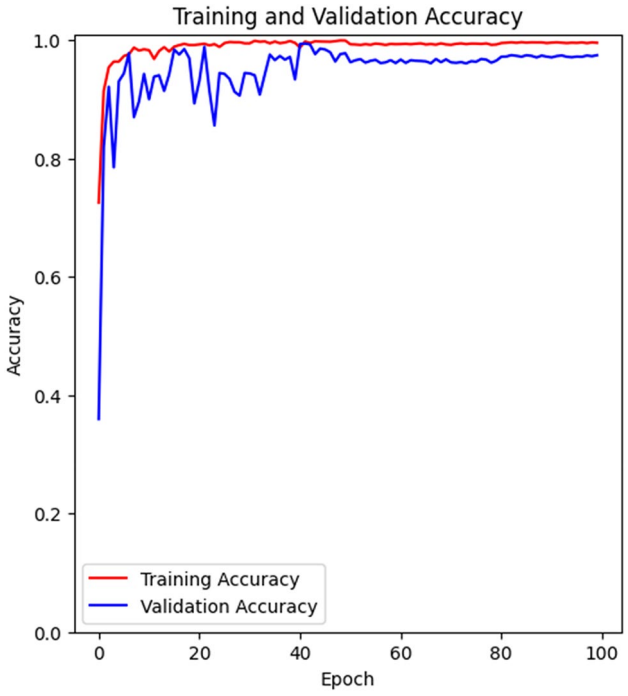

Fig. 14. EfficientNetB7- Attention -Accuracy.

The comparative analysis of various methods for the Figshare dataset for brain tumor detection is revealed in Table 9, an understanding of the effectiveness of different approaches. Classical machine learning methods such as Transfer Learning, SVM & KNN, and Partial Least Square demonstrate competitive accuracies around the 97–98% range, showcasing the robustness of these well-established techniques. Deep learning architectures, including CNNs, Vision Transformer (ViT), Vgg 16, and Alexnet, exhibit high accuracies, emphasizing the potency of deep neural networks in capturing intricate patterns within brain images. Attention mechanisms, as seen in Dual-Attention and Self Attention, contribute significantly to accuracy, highlighting the importance

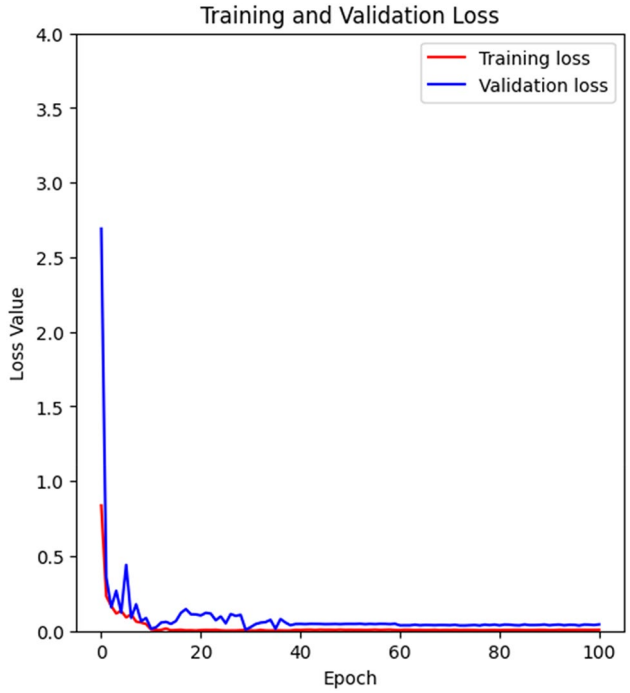

Fig. 15. Proposed Ensemble-Attention-Loss.

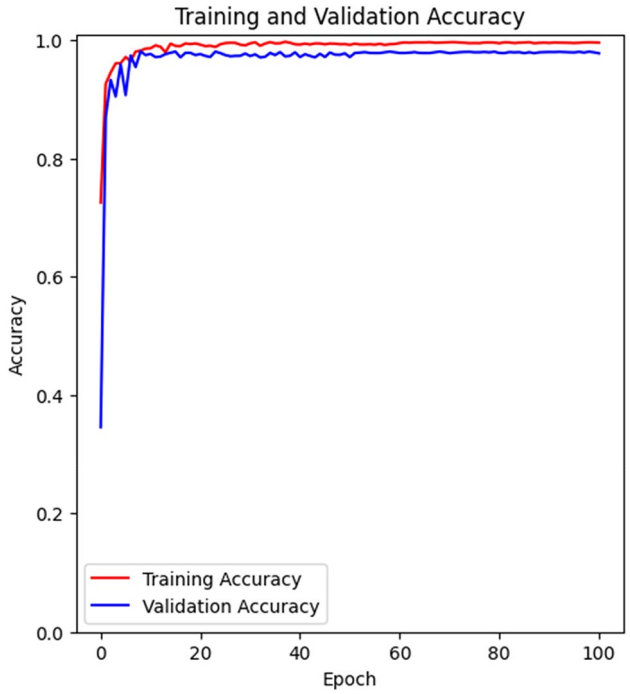

Fig. 16. Proposed Ensemble- Attention -Accuracy.

of focusing on critical image regions. Notably, the proposed Ensemble Attention model surpasses all other methods, achieving an outstanding accuracy of 98.94%. This suggests that combining attention mechanisms with an ensemble approach enhances the model's discriminative power, making it a promising method for the healthcare sector in brain tumor detection.

Table 10 compares the performance of various existing methods on the BraTs 2019 dataset in terms of accuracy. Different techniques such as Regular CNN, Multi-stream, Transfer Learning, Multi-scale, Cascaded CNN, Random Forest, spatial methods, and CNN are compared. The proposed Ensemble Attention method

Method	Accuracy	Precision	Recall	F1-Score	AUC
Majority voting	97.3	97.5	97.5	97.4	97
Weighted Averaging	97.9	97.91	97.95	97.93	97.8
Averaging	98.94	98.91	98.93	98.91	98.4

Table 3. Performance comparison of different ensemble techniques.

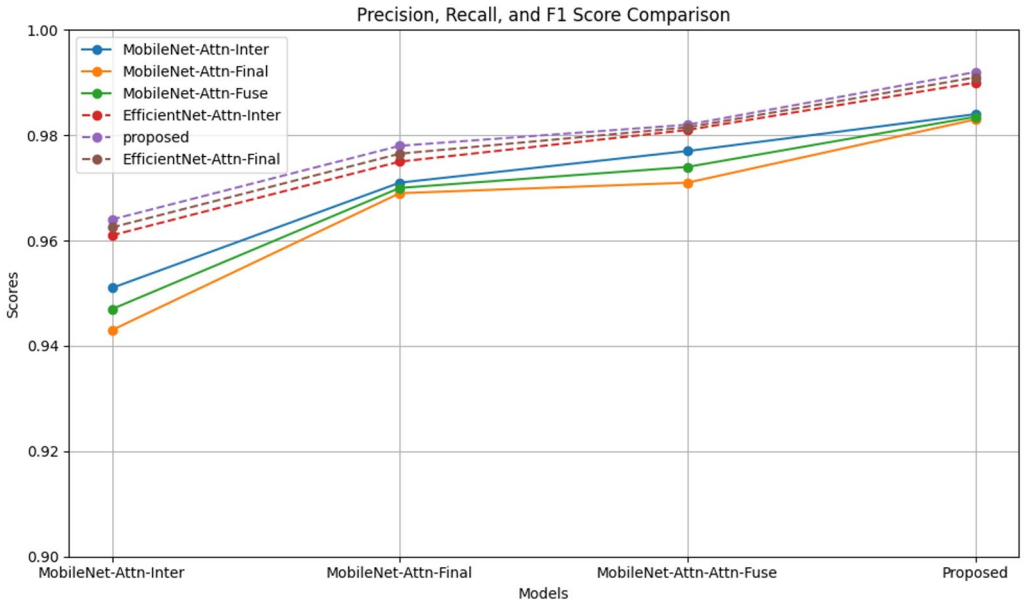

Fig. 17. Recall precision performance.

EfficientNet variants	Accuracy	Precision	Recall	F1-Score	AUC
EfficientNetB0 + EnsembleAttn	95.1	95.0	95.95	95.9	95.5
EfficientNetB1 + EnsembleAttn	95.9	95.7	95.8	95.9	95.2
EfficientNet B2 + EnsembleAttn	96.3	96.2	96.4	96.91	96.1
EfficientNet B3 + EnsembleAttn	96.9	96.8	96.6	96.91	96.4
EfficientNet B4 + EnsembleAttn	97.1	97.1	97.0	97.91	97.1
EfficientNet B5 + EnsembleAttn	97.5	97.2	97.3	97.91	97.2
EfficientNet B6 + EnsembleAttn	97.7	97.5	97.4	97.6	97.5
EfficientNet B7 + EnsembleAttn	97.91	97.91	97.6	97.90	97.8

Table 4. Performance of EfficientNet varieties with ensemble attention.

MobileNet Variants	Accuracy	Precision	Recall	F1-Score	AUC
MobileNetV1 + EnsembleAttn	94.9	94.5	94.5	94.9	94.8
MobileNetV2 + EnsembleAttn	96.2	96.3	96.4	96.1	96.2
MobileNetV3 + EnsembleAttn	97.1	97.2	97.3	97.11	97.3

Table 5. Performance of MobileNet varieties with ensemble attention.

achieved the highest accuracy among all methods listed in the table. The proposed ensemble attention method got superior performance in both figshare and the BraTS datasets, which proved the robustness of the proposed system.

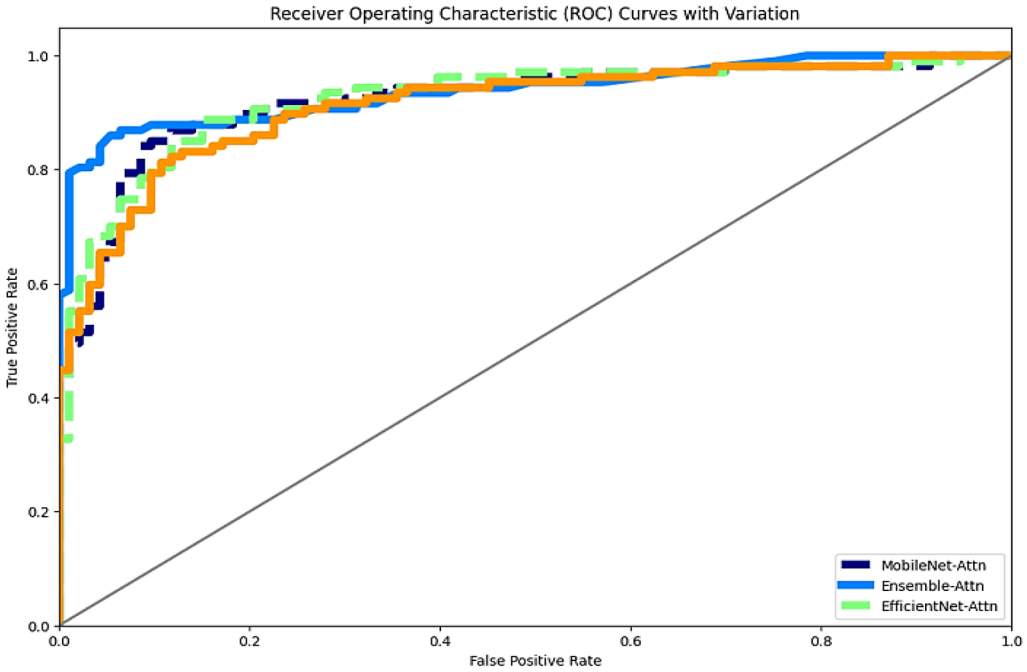

Fig. 18. ROC curve comparison.

Combination	Accuracy	AUC
MobileNetV3Attn + EfficientNetB7	95.8	95
MobileNetV3Attn_Inter + EfficientNetB7	96.9	96.1
MobileNetV3Attn_Final + EfficientNetB7	96.7	96.2
EfficientNetB7Attn + MobilNetV3	96.2	96.1
EfficientNetB7Attn_Inter + MobilNetV3	96.9	96.3
EfficientNetB7AttnFinal + MobilNetV3	97.1	97
Proposed (Ensemble)	98.94	98.1

Table 6. Different combinations of networks with attention.

Conclusions

In conclusion, the challenges associated with the precise identification of brain tumors in magnetic resonance imaging images, due to the diverse anatomical structures, are effectively addressed through the proposed innovative approach— the ensemble attention mechanism. This method employs two networks, utilizing MobileNetV3 and EfficientNetB7, to extract intermediate- and final-level feature maps. The incorporation of a co-attention mechanism at both intermediate and final feature map levels enhances the feature extraction stage, directing attention to specific regions and facilitating the extraction of global-level features at different model levels. The resulting ensemble of attentive feature maps significantly improves the detection of diverse patterns within brain tumor images at local and global levels, thereby enhancing the classification process.

The evaluation of this approach on the Figshare dataset yielded an impressive accuracy of 98.94% and 98.48% for the BraTs 2019 dataset surpassing the performance of other methods. This outcome underscores the efficacy of the proposed system for real-time brain tumor detection in healthcare systems. In the context of the global health concern posed by brain tumors, the innovative ensemble attention mechanism emerges as a promising and accurate tool for timely and effective detection, thereby contributing to the improvement of patient outcomes and overall quality of life.

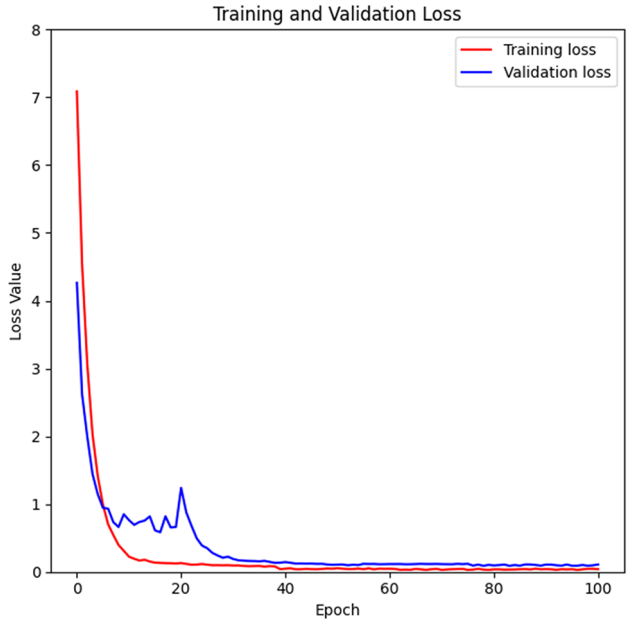

Fig. 19. Proposed Ensemble Attention-Loss- BraTs 2019.

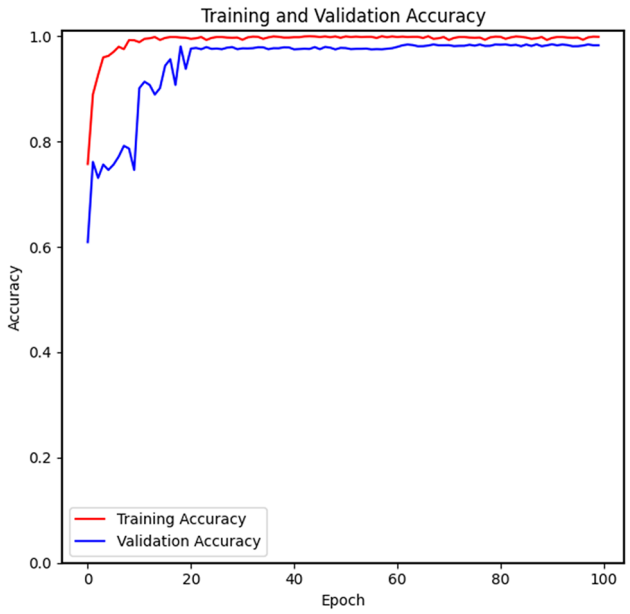

Fig. 20. Proposed Ensemble Attention –Accuracy-BraTs 2019.

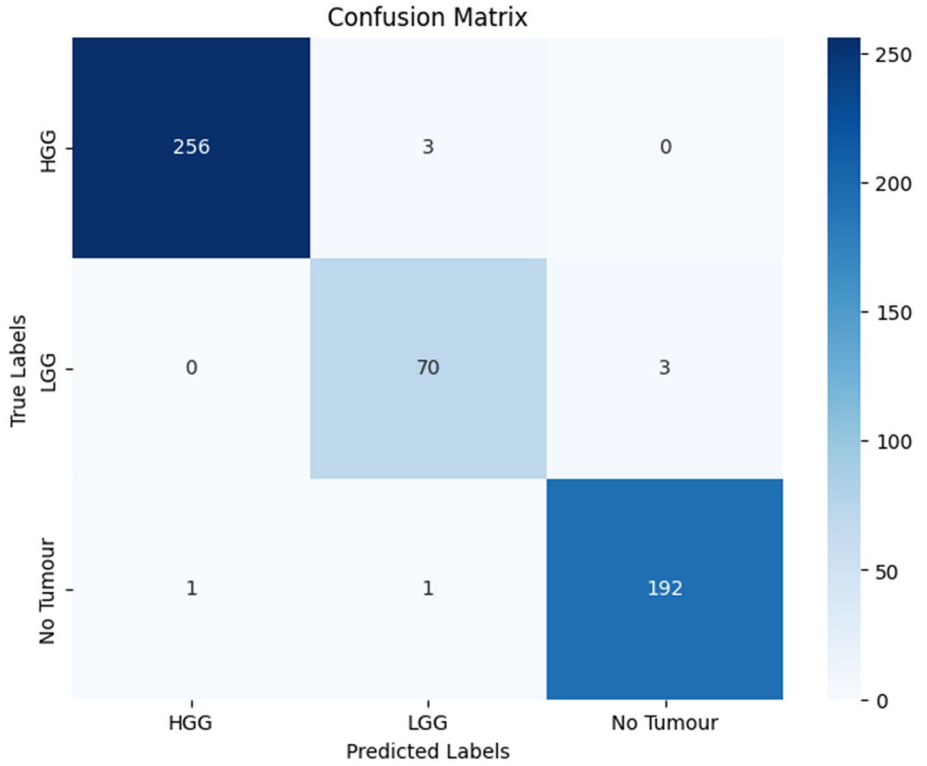

Fig. 21. Confusion matrix for BraTs 2019 Dataset.

Combination	Accuracy	AUC
MobileNetV3Attn + EfficientNetB7	95.2	94.9
MobileNetV3Attn_Inter + EfficientNetB7	96.5	96.2
MobileNetV3Attn_Final + EfficientNetB7	96.3	96.1
EfficientNetB7Attn + MobilNetV3	96	96.0
EfficientNetB7Attn_Inter + MobilNetV3	96.7	96.2
EfficientNetB7AttnFinal + MobilNetV3	97.01	97
Proposed (Ensemble)	98.28	98.1

Table 7. Different combinations of networks with attention- brats 2019.

With Ensemble	Accuracy
MobileNetV1 + EnsembleAttn	94.5
MobileNetV2 + EnsembleAttn	96.1
MobileNetV3 + EnsembleAttn	96.9
EfficientNetB0Attn + EnsembleAttn	94.9
EfficientNetB1Attn + EnsembleAttn	95.6
EfficientNetB2Attn + EnsembleAttn	96.2
EfficientNetB3Attn + EnsembleAttn	96.7
EfficientNetB4Attn + EnsembleAttn	97
EfficientNetB5Attn + EnsembleAttn	97.17
EfficientNetB6Attn + EnsembleAttn	97.23
EfficientNetB7Attn + EnsembleAttn	97.52

Table 8. Performance of MobileNet & EfficientNet varieties with ensemble Attention- BraTs 2019.

Reference	Method	Accuracy (%)
Deepak et al.[34]	Transfer learning	98
Öksüz et al.[49]	SVM & KNN	97.25
Pareek et al.[50]	Kernal based SVM	97
Alqudah et al.[51]	CNN	98.93
Tummala et al.[52]	ViT-image	98.7
Rehman et al.[47]	Vgg 16	98.69
Aamir et al.[53]	Partial least square	98.91
Díaz-Pernas[54]	DNN	97.3
Sarkar et al.[55]	Alexnet	98.15
Jun et al.[56]	Dual-attention	98.61
Salha et al.[58]	Self Attention	97.94
Proposed	**Ensemble Attention**	**98.94**

Table 9. Existing System Performance Comparison Figshare dataset.

Reference	Method	Accuracy (%)
Pei et al.9[63]	Regular CNN	74.9
Ge et al.[64]	Multi-stream	90.87
Yang et al.[12]	Transfer learning	94.5
Mzoughi et al.[65]	Multi-scale	96.49
Zhuge et al.[66]	Cascaded CNN	97.1
Ouerghi et al.[67]	Random Forest	96.5
Chatterjee[68]	Spatiospatial	96.98
Hafeez et al.[69]	CNN	97.85
Proposed	**Ensemble Attention**	**98.48**

Table 10. Existing system performance comparison BraTs 2019 dataset.

Data availability

The datasets used and/or analysed during the current study available from the corresponding author on reasonable request.

Received: 3 February 2024; Accepted: 20 September 2024
Published online: 27 September 2024

References

1. Louis, D. N. et al. The 2016 World Health Organization classification of tumors of the central nervous system: a summary. *Acta Neuropathol.* **131** (6), 803–820 (2016).
2. Bahadure, N. B., Ray, A. K. & Thethi, H. P. Image analysis for MRI based brain tumor detection and feature extraction using biologically inspired BWT and SVM, International Journal of Biomedical Imaging, vol. Article ID 9749108, 12 pages, 2017. (2017).
3. Pradhan, A. et al. On the classification of mr images using elm-ssa coated hybrid model. *Mathematics*. **9** (17), 2095 (2021).
4. Rasool, M. et al. A hybrid deep learning model for brain tumour classification. *Entropy*. **24** (6), 799 (2022).
5. Abd El-Wahab, B. S., Nasr, M. E., Khamis, S. & Ashour, A. S. Btc-fcnn: fast convolution neural network for multi-class brain tumor classification. *Health Inf. Sci. Syst.* **11** (1), 3 (2023).
6. Wang, S. et al. Towards updated understanding of brain metastasis. *Am. J. Cancer Res.* **12** (9), 4290–4311 (2022).
7. Vankdothu, R., Hameed, M. A. & Fatima, H. A brain tumor identification and classification using deep learning based on CNNLSTM method. *Comput. Electr. Eng.* **101**, 107960 (2022).
8. Asiri, A. A. et al. Novel inherited modeling structure of Automatic Brain Tumor Segmentation from MRI. *Comput. Mater. Contin.* **73**, 3983–4002 (2022).
9. Rosa, S. L. & Uccella, S. Pituitary tumors: Pathology and genetics. In Reference Module in Biomedical Sciences; Elsevier: Amsterdam, The Netherlands, (2018).
10. Ayadi, W., Elhamzi, W., Charfi, I. & Atri, M. Deep CNN for Brain Tumor classification. *Neural Process. Lett.* **53**, 671–700 (2021).
11. Jayade, S., Ingole, D. T. & Ingole, M. D. Review of Brain Tumor Detection Concept using MRI Images. In Proceedings of the 2019 International Conference on Innovative Trends and Advances in Engineering and Technology (ICITAET), Shegoaon, India, 27–28 December 2019.
12. Yang, Y. et al. Glioma grading on conventional MR images: a deep learning study with transfer learning. *Front. Neurosci.* **12**, 804 (2018).
13. Nazir, M., Shakil, S. & Khurshid, K. Role of deep learning in brain tumor detection and classification (2015 to 2020): a review. *Comput. Med. Imaging Graph.* **91**, 101940 (2021).
14. El-Kenawy, E. S. M. et al. Meta-heuristic optimization and Keystroke Dynamics for Authentication of Smartphone Users. *Mathematics*. **10**, 2912 (2022).
15. El-kenawy, E. S. M. et al. Feature selection and classification of transformer faults based on Novel Meta-Heuristic Algorithm. *Mathematics*. **10**, 3144 (2022).

16. El-Kenawy, E. S. M. et al. Novel Meta-heuristic algorithm for feature selection, unconstrained functions and Engineering problems. *IEEE Access.* **10**, 40536–40555 (2022).
17. Gurusamy, R. & Subramaniam, V. A machine learning approach for MRI brain tumor classification. *Comput. Mater. Contin.* **53**, 91–109 (2017).
18. Ramdlon, R. H., Kusumaningtyas, E. M. & Karlita, T. Brain Tumor Classification Using MRI Images with K-Nearest Neighbor Method. In Proceedings of the 2019 International Electronics Symposium (IES), Surabaya, Indonesia, 27–28 September ; pp. 660–667. [CrossRef] (2019).
19. Sajjad, M. et al. Multi-grade brain tumor classification using deep CNN with extensive data augmentation. *J. Comput. Sci.* **30**, 174–182 (2019).
20. Ding, Y. et al. Classification of alzheimer's disease based on the combination of morphometric feature and texture feature, in 2015 IEEE International Conference on Bioinformatics and Biomedicine (BIBM), pp. 409–412, IEEE (2015).
21. Ahmad, I. et al. Efficient algorithms for e-healthcare to solve multiobject fuse detection problem. *J. Healthc. Eng.* **2021**, 1–16 (2021).
22. Ahmad, I., Liu, Y., Javeed, D. & Ahmad, S. A decision-making technique for solving order allocation problem using a genetic algorithm, in IOP Conference Series: Materials Science and Engineering, vol. 853, p. 012054, IOP Publishing (2020).
23. Binaghi, E. et al. Automatic segmentation of mr brain tumor images using support vector machine in combination with graph cut. *IJCCI (NCTA)* 152–157 (2014).
24. Cheng, J. et al. Enhanced performance of brain tumor classification via tumor region augmentation and partition. *PloS One.* **10** (10), e0140381 (2015).
25. Sajid, S., Hussain, S. & Sarwar, A. Brain tumor detection and segmentation in MR images using deep learning. *Arab. J. Sci. Eng.* **44** (11), 9249–9261 (2019).
26. Saxena, P., Maheshwari, A. & Maheshwari, S. Predictive modeling of brain tumor: a deep learning approach, in Innovations in Computational Intelligence and Computer Vision. Advances in Intelligent Systems and Computing, vol 1189Springer, Singapore.
27. Çinar & Yildirim, M. Detection of tumors on brain MRI images using the hybrid convolutional neural network architecture.
28. Khawaldeh, S., Pervaiz, U., Rafiq, A. & Alkhawaldeh, R. S. Noninvasive grading of glioma tumor using magnetic resonance imaging with convolutional neural networks. *Appl. Sci.* **8** (1), 27 (2018).
29. Preethi, S. & Aishwarya, P. Combining wavelet texture features and deep neural network for tumor detection and segmentation over MRI. *J. Intell. Syst.* **28** (4), 571–588 (2019).
30. Hemanth, D. J. et al. A modified deep convolutional neural network for abnormal brain image classification. *IEEE Access.* **7**, 4275–4283 (2019).
31. Khan, M. A. et al. Multimodal brain tumor classification using deep learning and robust feature selection: a machine learning application for radiologists. *Diagnostics.* **10** (8), 565 (2020).
32. Guan, Y. et al. A framework for efficient brain tumor classification using mri images, (2021).
33. Badža, M. M. & Barjaktarović, M. Č. Classification of brain tumors from mri images using a convolutional neural network. *Appl. Sci.* **10** (6), 1999 (2020).
34. Deepak, S. & Ameer, P. Brain tumor classification using deep cnn features via transfer learning. *Comput. Biol. Med.* **111**, 103345 (2019).
35. Gumaei, A., Hassan, M. M., Hassan, M. R., Alelaiwi, A. & Fortino, G. A hybrid feature extraction method with regularized extreme learning machine for brain tumor classification. *IEEE Access.* **7**, 36266–36273 (2019).
36. Zhang, Y., Dong, Z., Wu, L. & Wang, S. A hybrid method for MRI brain image classification. *Expert Syst. Appl.* **38**, 10049–10053 (2011).
37. Arakeri, M. P. & Reddy, G. R. M. Computer-aided diagnosis system for tissue characterization of brain tumor on magnetic resonance images. *Signal. Image Video Process.* **9**, 409–425 (2015).
38. Jayachandran, A. & Dhanasekaran, R. Severity Analysis of Brain Tumor in MRI images using modified Multitexton structure Descriptor and Kernel-SVM. *Arab. J. Sci. Eng.* **39**, 7073–7086 (2014).
39. El-Dahshan, E. S. A., Hosny, T. & Salem A.-B.M. Hybrid intelligent techniques for MRI brain images classification. *Digit. Signal. Process.* **20**, 433–441 (2010).
40. Khazaee, Z., Langarizadeh, M. & Ahmadabadi, M. E. S. Developing an Artificial Intelligence Model for Tumor Grading and classification, based on MRI sequences of human brain gliomas. *Int. J. Cancer Manag.* **15**, e120638 (2022).
41. Ye, N. et al. Classification of Gliomas and Germinomas of the basal ganglia by transfer learning. *Front. Oncol.***12**, 844197 (2022).
42. Amou, M. A., Xia, K., Kamhi, S., Mouhafid, M. A. & Novel MRI diagnosis method for brain tumor classification based on CNN and bayesian optimization. *Healthcare.* **10**, 494 (2022). [CrossRef] [PubMed].
43. Alanazi, M. et al. Brain Tumor/Mass Classification Framework Using Magnetic-Resonance-Imaging-Based Isolated and Developed Transfer Deep-Learning Model. *Sensors* **22**, 372. (2022). [CrossRef] [PubMed].
44. Rizwan, M. et al. Brain tumor and Glioma Grade classification using gaussian convolutional neural network. *IEEE Access.* **10**, 29731–29740 (2022).
45. Isunuri, B. V. & Kakarla, J. Three-class brain tumor classification from magnetic resonance images using separable convolution-based neural network. *Concur. Comput. Pract. Exp.* **34**, e6541 (2021).
46. Kaur, T. & Gandhi, T. K. Deep convolutional neural networks with transfer learning for automated brain image classification. *J. Mach. Vis. Appl.* **31**, 20 (2020).
47. Rehman, A., Naz, S., Razzak, M. I., Akram, F. & Imran, M. A. Deep learning-based Framework for Automatic Brain tumors classification using transfer learning. *Circuits Syst. Signal. Process.* **39**, 757–775 (2019).
48. Deepa, S., Janet, J., Sumathi, S. & Ananth, J. P. Hybrid optimization Algorithm enabled Deep Learning Approach Brain Tumor segmentation and classification using MRI. *J. Digit. Imaging.* **36**, 847–868 (2023).
49. Öksüz, C., Urhan, O. & Güllü, M. K. Brain tumor classification using the fused features extracted from expanded tumor region. *Biomed. Signal. Process. Control.* **72**, 103356 (2022).
50. Pareek, M., Jha, C. K. & Mukherjee, S. Brain tumor classification from MRI images and calculation of Tumor Area. In Advances in Intelligent Systems and Computing; Springer: Singapore, ; 73–83 (2020). ._7.
51. Alqudah, A. M., Alquraan, H., Qasmieh, I. A., Alqudah, A. & Al-Sharu, W. Brain tumor classification using deep learning technique—a comparison between cropped, uncropped, and segmented lesion images with different. *Int. J. Adv. Trends Comput. Sci. Eng.* **8** (6), 3684–3691 (2019).
52. Tummala, S., Kadry, S., Bukhari, S. A. C. & Rauf, H. T. Classification of brain tumor from magnetic resonance imaging using Vision transformers Ensembling. *Curr. Oncol.* **29**, 7498–7511 (2022).
53. Aamir, M. et al. A deep learning approach for brain tumor classification using MRI images. *Comput. Electr. Eng.* **101** (1), 1–21 (2022).
54. Díaz-Pernas, F. J., Martínez-Zarzuela, M. & Antón-Rodríguez, M. González-Ortega, D. A deep learning approach for brain tumor classification and segmentation using a multiscale convolutional neural network. *Feature Papers Artif. Intell. Med.* **9** (2), 1–14 (2021).
55. Sarkar, A., Maniruzzaman, M. A. & Alahe, M. A. An effective and novel approach for brain tumor classification using AlexNet CNN feature extractor and multiple eminent machine learning classifiers in MRIs. *J. Sens. Hindawi.* **1224619**, 1–19 (2023).
56. Jun, W. & Liyuan, Z. Brain tumor classification based on attention guided Deep Learning Model. *Int. J. Comput. Intell. Syst.* **15**, 35. https://doi.org/10.1007/s44196-022-00090-9 (2022).

57. Mitra, A., Tripathi, P. C. & Bag, S. Identification of Astrocytoma Grade using intensity, texture, and shape based features. In: (eds Das, K., Bansal, J., Deep, K., Nagar, A., Pathipooranam, P. & Naidu, R.) Soft Computing for Problem Solving. Advances in Intelligent Systems and Computing, vol 1048. Springer, Singapore. https://doi.org/10.1007/978-981-15-0035-0_36 (2020).
58. Salha, M. & Alzahrani ConvAttenMixer: Brain tumor detection and type classification using a convolutional mixer with external and self-attention mechanisms, Journal of King Saud University - Computer and Information Sciences, Volume 35, Issue 10,2023.
59. Tripathi, P. C. & Bag, S. Non-invasively Grading of Brain Tumor through noise robust textural and intensity based features. In: (eds Das, A., Nayak, J., Naik, B., Pati, S. & Pelusi, D.) Computational Intelligence in Pattern Recognition. Advances in Intelligent Systems and Computing, vol 999. Springer, Singapore. https://doi.org/10.1007/978-981-13-9042-5_45. (2020).
60. Bakas, S. et al. Identifying the best machine learning algorithms for brain tumor segmentation, progression assessment, and overall survival prediction in the brats challenge. *arXiv Preprint arXiv* :181102629 (2018).
61. Tripathi, P. C. & Bag, S. A computer-aided grading of glioma tumor using deep residual networks fusion,Computer Methods and Programs in Biomedicine,215, 2022 106597,ISSN 0169–2607 https://doi.org/10.1016/j.cmpb.2021.106597
62. Tripathi, P. C., Bag, S., An Attention-Guided, C. N. N. & Framework for Segmentation and Grading of Glioma Using 3D MRI Scans. IEEE/ACM Trans Comput Biol Bioinform. doi: (2023). May-Jun;20(3):1890–1904 https://doi.org/10.1109/TCBB.2022.3220902. Epub 2023 Jun 5. PMID: 36350865.
63. Pei, L. et al. Brain tumor classification using 3d convolutional neural network. *Int. MICCAI Brain Lesion Workshop*, 335–342 (2019).
64. Ge, C. et al. Deep learning and multi-sensor fusion for glioma classification using multistream 2d convolutional networks. In. 40th Annual International Conference of the IEEE Engineering in Medicine and Biology Society (EMBC), 5894–5897 (2018). (2018).
65. Mzoughi, H. et al. Deep multi-scale 3d convolutional neural network (cnn) for mri gliomas brain tumor classification. *J. Digit. Imaging.* **33**, 903–915 (2020).
66. Zhuge, Y. et al. Automated glioma grading on conventional mri images using deep convolutional neural networks. *Med. Phys.* **47**, 3044–3053 (2020).
67. Ouerghi, H. et al. Glioma classification via mr images radiomics analysis. Vis. Comput. 1–15 (2021). (2021).
68. Chatterjee, S. et al. Classification of brain tumours in MR images using deep spatiospatial models. *Sci. Rep.* **12**, 1505. https://doi.org/10.1038/s41598-022-05572-6 (2022).
69. Hafeez, H. A. et al. A CNN-Model to Classify Low-Grade and High-Grade Glioma From MRI Images, in IEEE Access, vol. 11, pp. 46283–46296, doi: (2023). https://doi.org/10.1109/ACCESS.2023.3273487

Author contributions

1,Fatih CELIK: Data curation, Software, Writing – original draft, Visualization, Investigation, Validation. 2,Kemal CELIK: Conceptualization, Methodology, Writing – original draft, Investigation, Supervision. 3,Ayse CELIK: Software, Investigation, Supervision, Writing – review & editing.4,All authors have read and agreed to the published version of the manuscript.

Funding

This research received no external funding.

Declarations

Competing interests

The authors declare no competing interests.

Additional information

Correspondence and requests for materials should be addressed to F.C.

Reprints and permissions information is available at www.nature.com/reprints.

Publisher's note Springer Nature remains neutral with regard to jurisdictional claims in published maps and institutional affiliations.